Turkish Journal of Earth Sciences (Turkish J. Earth Sci.), Vol. 17, 2008, pp. 763–784. *Copyright ©TÜBİTAK*
First published online: 13 March 2008

Quaternary Calcrete Development in the Mersin Area, Southern Turkey

MUHSİN EREN[1], SELAHATTİN KADİR[2], ZÜBEYDE HATİPOĞLU[1] & MURAT GÜL[3]

[1] Mersin Üniversitesi, Mühendislik Fakültesi, Jeoloji Mühendisliği Bölümü, Çiftlikköy, TR–33343 Mersin, Turkey
(e-mail: m_eren@yahoo.com)

[2] Eskişehir Osmangazi Üniversitesi, Mühendislik Mimarlık Fakültesi, Jeoloji Mühendisliği Bölümü,
Meşelik, TR–26480 Eskişehir, Turkey

[3] Muğla Üniversitesi, Mühendislik Fakültesi, Jeoloji Mühendisliği Bölümü, Kötekli, TR–40000 Muğla, Turkey

Abstract: Quaternary calcretes are widespread in the Mersin area and occur in a variety of forms. Several distinct calcrete profiles are recognized and subdivided into two major groups defined by mature and immature profiles. Mature calcrete profiles comprise a generally isolated calcrete horizon at the base and hard laminated crust at the top with rarely pisolithic crust in the uppermost part. The immature calcrete profiles consist mainly of an isolated calcrete horizon which is rarely overlain by a laminated crust. Calcrete forms show three main stages of development: (i) a mottled or plugged horizon, comprising isolated calcrete forms such as powdery, nodule, tube, and fracture-fill; (ii) calcareous crusts, including laminar and hard laminated calcrete crusts, and (iii) a pisolithic crust which is very restricted. The plugged horizon, in which calcite is precipitated from downward moving percolating water, reduces the permeability of the host-rocks. Later, the plugged horizon leads to the horizontal movement of percolating water with formation of a calcareous crust. Finally, a pisolithic crust forms by down-slope movement of the grains and their accumulation in troughs between dome-like structures. XRD, ICP-AES and SEM analyses show that calcrete samples are composed predominantly of calcite, and palygorskite is closely associated with them as a minor constituent. Calcite $\delta^{18}O$ and $\delta^{13}C$ isotope values of calcrete samples vary between –4.31 to –6.82 and –6.03 to –9.65 ‰ PDB, respectively which indicates formation from percolating meteoric water at, or near to, the surface and supporting a thin column of soil. Abundance of beta fabric constituents and negative calcite $\delta^{13}C$ values suggest a pedogenic origin for the calcretes. They appear to have formed from percolating soil-derived water mainly by precipitation and replacement, and also by displacive replacement (detrital grain calcification) and biomineralization under alternating wet and dry climatic conditions.

Key Words: calcrete, hardpan, nodule, pedogenesis, Quaternary, Turkey

Mersin Yöresinde (Güney Türkiye) Kuvaterner Kaliş Gelişimi

Özet: Mersin yöresinde, Kuvaterner kalişler yaygındır ve değişik şekillerde oluşur. Yörede birkaç belirgin kaliş profili ayırt edilirken, olgun ve olgunlaşmamış profiller olarak başlıca iki alt gruba ayrılırlar. Olgun kaliş profilleri genellikle tabanda ayrık kaliş seviyesinden ve üstte sert laminalı kabuktan, ve nadiren en üstte pizolitik kabuktan oluşur. Olgunlaşmamış kaliş profilleri başlıca ayrık kaliş seviyesinden oluşur ve oldukça yersel alanlarda nadiren laminalı kabuk tarafından üzerlenir. Kaliş şekilleri arazide üç gelişim evresi gösterir: (i) toz, yumru, tüp ve çatlak dolgusu gibi ayrık kaliş şekilleri içeren lekeli veya geçirimsiz seviye; (ii) laminalı ve sert laminalı kaliş kabuk seviyelerini içeren kireçli kabuklar; ve (iii) oldukça sınırlı pizolitik kabuk. Kalsitin aşağı sızan sulardan çökeldiği geçirimsiz seviye ana kayaç veya çökellerin geçirimliliğini azaltmıştır. Daha sonra, geçirimsiz seviye sızan suların yatay hareketine öncülük yapmış, bu yüzden kireçli kabuklar oluşmuştur. Son olarak pizolitik kabuk tanelerin yamaç aşağı hareketi ve onların domsu yapılar arasındaki çukurluklarda yığışmasıyla oluşmuştur. XRD, ICP-AES ve SEM analizleri kaliş örneklerinin hakim olarak kalsitten meydana geldiğini ve paligorskitin onlarla küçük bileşen olarak sıkı bir şekilde bulunduğunu gösterir. Kaliş örneklerinin kalsit $\delta^{18}O$ ve $\delta^{13}C$ izotop değerleri sırasıyla –4.31 ile –6.82 ve –6.03 ile –9.65 ‰ PDB arasında değişir. Bu değerler yüzeyde veya yüzeye yakın ince toprak örtüsü altında sızan tatlı sudan oluşumu gösterir. Beta doku bileşenlerinin bolluğu ve negatif kalsit $\delta^{13}C$ değerleri kalişler için pedojenik kökeni önerir. Kalişler, tekrarlanan nemli ve kurak iklim koşulları altında, sızan toprak kökenli sulardan başlıca çökelim ve ornatmayla, ve ayrıca yer değiştiren ornatım (detrital tane kalsitleşmesi) ve biyomineralleşme ile oluşmuştur.

Anahtar Sözcükler: kaliş, sert kabuk, yumru, toprak oluşumu, Kuvaterner, Türkiye

Introduction

The term 'calcrete' (synonymous caliche) describes a near-surface, terrestrial accumulation of predominantly calcium-carbonate ($CaCO_3$) in unconsolidated sediments, sedimentary rocks and soils (Goudie 1973, 1983, 1996; Watts 1980; Wright & Tucker 1991; Demicco & Hardie 1994; Wright *et al*. 1995; Khadkikar *et al*. 1998). It occurs in a variety of forms from powdery to nodular to highly indurated crust (hardpan) (Esteban & Klappa 1983; Goudie 1983, 1996; Wright & Tucker 1991). Calcrete is characteristic of arid and semi-arid climates under which rainfall is between 200 and 600 mm per year with evaporation exceeding this precipitation, and with a mean annual temperature of about 18 °C (James 1972; Goudie 1973, 1983; Hay & Reeder 1978; Tucker 1991; Lal & Kimble 2000; Flugel 2004). There are two fundamentally different models to explain the formation of calcrete: (i) the per descensum model (pedogenic calcrete) based on downward movement of dissolved $CaCO_3$, and (ii) the per ascensum model (groundwater calcrete) related to the capillary rise of groundwater (Goudie 1973, 1983).

The study area is situated in Mersin, a city near the Mediterranean Sea in southern Turkey (Figure 1). The climate is semi-arid with a mean annual precipitation of 634 mm, a mean annual evaporation of 1321 mm and an average annual temperature of 18.7 °C based on 70 years of meteorological records. The suitable climatic conditions with the other factors have resulted in an extensive calcrete formation in the Mersin area. Despite widespread occurrence, previous calcrete studies in the region and in Turkey are very limited. These studies describe variations in calcretes with toposequences and their evolution in the Adana Basin (Kapur *et al*. 1990) and in southern Anatolia (Atalay 1996; Kapur *et al*. 2000), calcretes in the Misis area of the Adana Basin (Kapur *et al*. 1993) and in the Kırşehir region (Atabey *et al*. 1998), and micromorphology of calcrete columns in the Adana Basin (Kapur *et al*. 1987). Calcretes in the Adana region are found on two terraces: the lower terrace (TL) with a height of less than 50 m shows only softpan calcretes, whereas the higher terrace (TH) with a height of 50–200 m, generally has hardpan and softpan calcretes together (Kapur *et al*. 1990, 2000; Atalay 1996). Özer *et al*. (1989) provide ESR (electron spin resonance) and TL (thermoluminescene) age determination of calcrete nodules from different places of Turkey, including the Adana region, and conclude that calcretes are older than 350 ka BP. Later, Atalay (1996) proposed a Pleistocene to Early Holocene age for the calcretes. Kapur *et al*. (1990) suggest six evolutionary stages for calcretes in the Adana region: (1) deposition of clays, (2) cracking of argillaceous material and formation of large cuboidal structural units, (3) leaching in wet periods and calcification along vertical continuations of structural units, (4) development of vertical columns and formation of overlying calcareous soil, (5) decalcification of soil and calcification along with rubefaction of the column horizon resulting in formation of a massive calcrete, (6) rubefaction with a thin crust forming over the massive calcrete. The present paper describes calcrete formation in the Mersin area and provides evidence for its origin with field data providing an important indication that formation occurs from downward moving water.

Geological Setting

The study area is on the western flank of the Adana Basin (Figure 1a) which is one of the major Neogene basins in the Tauride orogenic belt (Yalçın & Görür 1983). In the basin, a thick sedimentary package ranging in age from Burdigalian to Recent unconformably overlies Palaeozoic and Mesozoic basement rocks (Yetiş 1988; Yetiş *et al*. 1995). In the study area Tertiary and Quaternary units are present (Figures 2 & 3). The Tertiary units are the Karaisalı Formation (Burdigalian–Early Serravalian), the Güvenç Formation (Burdigalian–Serravalian) and the Kuzgun Formation (Tortonian). The Quaternary units comprise a hard laminated crust (hardpan calcrete), deltaic deposits, pebbly alluvial red soils (colluvium) and recent alluvium/terrace deposits. Calcrete formation is widespread in and over the Kuzgun Formation especially in red mudstone and also occurs in the alluvial red soils.

Materials and Methods

Different calcrete forms and profiles were described in the field and eighty calcrete samples and twenty host-rock and sediment samples were collected from a number of different outcrops. Thin-sections were prepared from indurated calcrete samples and examined by optical microscope. X-ray powder diffraction (XRD) was used to determine bulk mineralogy of most samples with analyses carried out using a Rigaku-Geigerflex diffractometer with Cu$K\alpha$ radiation and a scanning speed of 1° 2θ/min at the General Directorate of Mineral Research and Exploration (MTA), Ankara, Turkey. Semi-quantitative estimates of

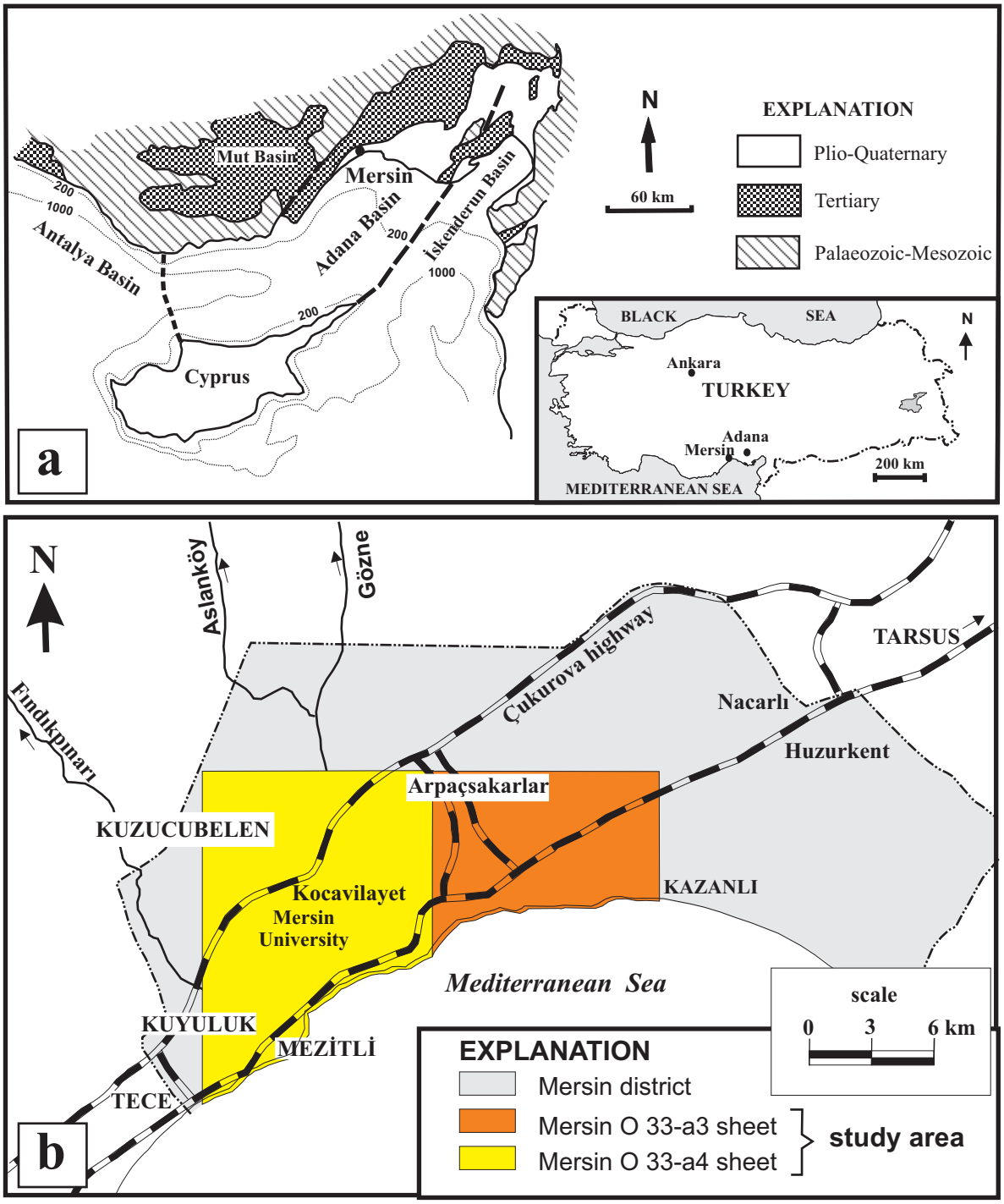

Figure 1. Location maps showing (a) the Adana Basin and (b) the study area.

rock-forming minerals were obtained by using the external standart method of Brindley (1980), whereas the relative abundance of clay-mineral fractions was determined using their basal reflections and the mineral intensity factors of Moore & Reynolds (1989). Scanning electron microscopy and energy-dispersive analyses (SEM-EDX) were performed at the Middle East Technical University, Ankara, Turkey using a JEOL JSM 84A instrument equipped with

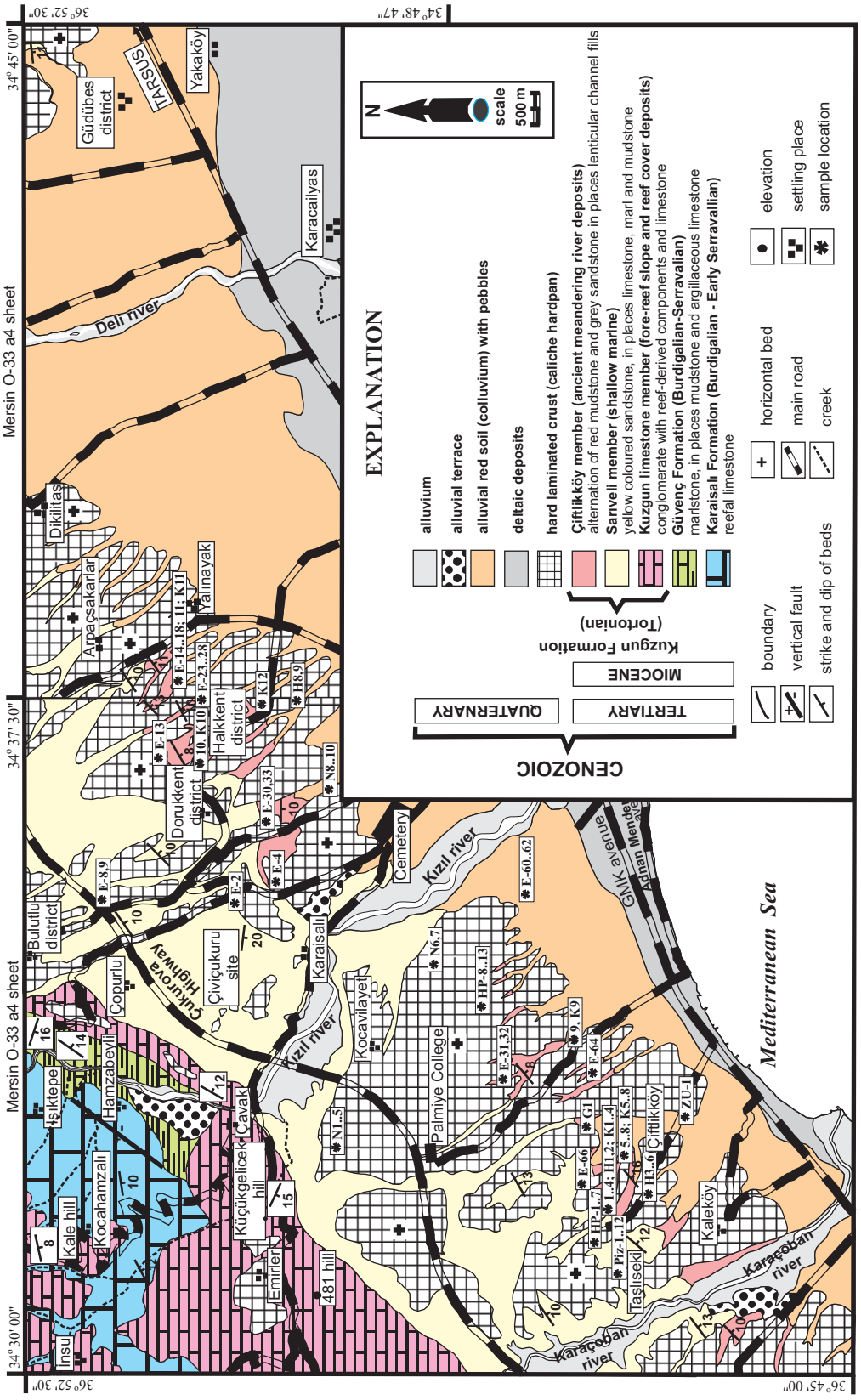

Figure 2. Geological map of the study area.

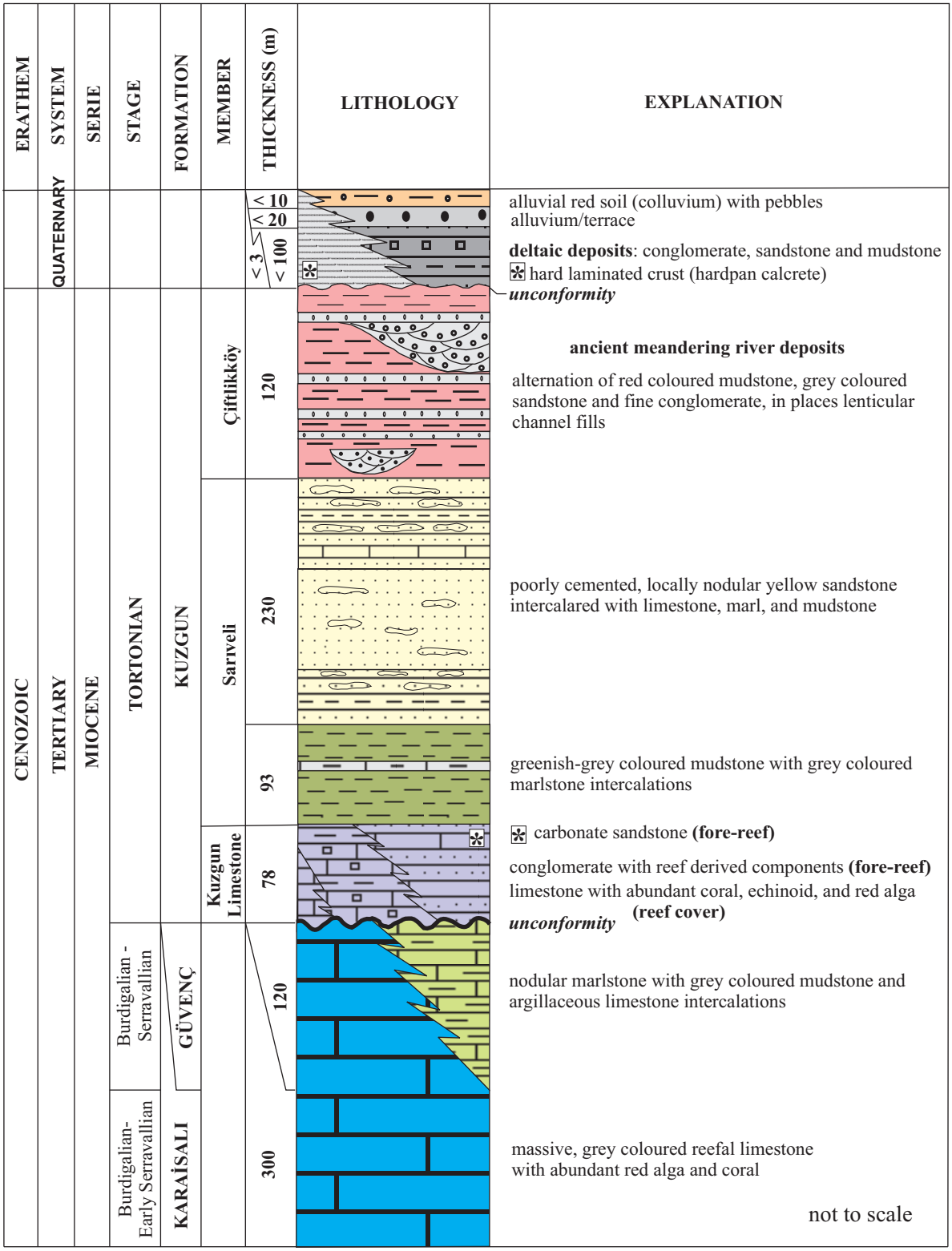

Figure 3. Generalized stratigraphical column of the study area.

an EDX detector. For SEM-EDX analysis, representative samples were prepared by adhering the fresh, broken surface of the sample onto an aluminium sample holder with double-sided tape and thinly coating with a film (~350 Å) of gold using a Giko ion coater. Chemical compositions of the selected samples were determined using inductively coupled plasma atomic emission spectroscopy (ICP-AES) at the ACME Analytical Laboratories Ltd., Vancouver, BC Canada. In the analyses, detection limits range from 0.01 to 0.1 wt% for major elements and 0.1 to 5 ppm for trace elements. Carbon and oxygen isotopes were determined using a Finigan MAT 252 mass spectrometer at the Southern Methodist University (SMU) laboratories, Dallas, TX, USA. 5–10 mg powdered calcrete samples were reacted with 100% phosphoric acid (H_3PO_4) at 50 °C. Replicate analyses on the randomly selected samples give a mean deviation of ± 0.05 ‰ for oxygen and ± 0.02 ‰ for carbon. All isotope data are reported in parts per mil (‰) with respect to the PDB standard.

Calcrete Formation in the Mersin Area

Field Description

In the Mersin area, calcrete occurrences are widespread and appear in a variety of forms such as powdery, nodular, tubular, fracture-fill, laminar crust, hard laminated crust (hardpan), pisolithic crust in and/or over the Kuzgun Formation of Tortonian age and Quaternary alluvial red soil (colluvium) (Figure 4). The most common calcrete types are hard laminated crust, nodular, tubular and fracture-filling forms. In the field, calcrete profiles vary from place to place. Therefore, several distinct calcrete profiles have been described and sketched in Figure 5.

Calcrete Types

Pisolithic crust is only found in one restricted place at the Taşlıseki site where two pisolithic beds with a thickness of 30 and 40 cm overlie hard laminated crust with an erosional surface (Figure 4a, b). Fragments of the pisolithic crust and pisoliths are also observed in some places. Pisoliths are inversely graded, poorly sorted, brown in colour, and spherical to subspherical in shape with a size of 2 mm to 6 cm.

Hard laminated crust (hardpan calcrete; Figure 4c–f) occupies large areas (Figure 2) in the region and appears as a wavy crust on small ridges and highs (ridge calcretes named by Rossinsky & Wanless 1992) in low topographic areas with heights of 20 to 250 m. It is often associated with root casts and traces. In some cases root mat (Figure 4k) and residual soil are observed within the hardpan. The hardpan predominantly overlies different rock types of the Kuzgun Formation with angular unconformity, and in some cases, remains of alluvial materials occur in erosional troughs. The hardpan is typically cream coloured, evenly and discontinuously laminated, indurated, wavy horizons of calcium carbonate with an average thickness of 1–1.5 m. It has a sharp upper surface and grades down through softer or isolated calcrete with nodules, tubes and fracture fills within red mudstone (the latter comprises overbank deposits of an ancient meandering river in the Kuzgun Formation; Figure 4c–e). The upper surface commonly shows dome-like morphologies interpreted as tepee-structures or pseudo-anticlines (Eren 2007), with troughs between them. Small-scale karstic features of karrens are often associated with the dome-like structures. In places, there is a thin soil cover over the hard laminated crust.

Laminar crust (?) is very restricted in the Mersin area, being exposed only in roadcuts of the İsmet İnönü avenue (Figure 4h). It is a loose to semi-indurated, dirty-cream coloured, laminated sheet of calcium carbonate formed immediately below the vegetation cover in the alluvial red soil. The crust can be followed for approximately 15 m in length and 25 to 90 cm in thickness. The laminar crust passes gradually downward into a nodular and tubular horizon. In this horizon, calcrete nodules and tubes become closer and coalesce upward to form a crust (Figure 4h).

Calcrete nodules are very common especially in overbank deposits (red coloured claystone or mudstone) of the Kuzgun Formation (Figure 4c–e) and alluvial red soils (Figure 4g, h). They are also rarely present in marine mudstones in green and yellow colours and grey coloured marlstones of the Kuzgun Formation. The nodular horizon often grades upward into the hard laminated crust and is commonly associated with calcrete tubes. Calcrete nodules are semi indurated, white coloured, crudely spherical to irregular or ellipsoid in shape, often isolated and, in some places, coalesced in arrangement. The nodule size ranges dominantly from 4 cm to 15 cm and occassionally up to 40 cm. Mudstone relics are often seen at the centre of the nodules (Figure 4i).

Calcrete tubes are a common form in the Mersin area and are closely associated with nodules in overbank deposits (red coloured mudstone) of the Kuzgun

Formation (Figure 4d, e) and with red alluvial soil (Figure 4g, h). They are semi-indurated, white-coloured, vertically to subvertically-oriented, in shapes of elongated lenses with a width of 4–10 cm and length from 20 cm to 1.5 m.

Calcrete powder is an early stage or nuclei for nodular calcrete, and is observed as a white coloured, finely crystalline, loose powder of calcium carbonate, especially in alluvial soil (Figure 5b1) fractured by desiccation. Powder is commonly associated with nodular and tubular forms.

Calcrete fracture fill (Figure 5a-2) is made up by semi-indurated, white-coloured calcium carbonate fills in non-tectonic fractures within the red mudstones of overbank deposits (the Kuzgun Formation) and appears in different forms as a honeycomb structure consisting of calcium carbonate filled thin fractures (Figure 4j) and interstitial mudstone areas among them at the bottom of hardpan, pseudo-folds below the hardpan (Figure 5a-2), and undulating fractures extending subparallel to the bed-dipping direction.

Calcrete Profiles

In the Mersin area, several distinct calcrete profiles are described in and/or over the Kuzgun Formation and alluvial red soils (Figure 5). Their thickness ranges from 0.5 m to 4.5 m. There are two main types of calcrete profile: (i) a maturate calcrete profile developed in and over the Kuzgun Formation (Figure 5a), and (ii) an immature calcrete profile which lacks the mainly hard laminated crust and is formed in the alluvial red soil (Figure 5b). Maturate calcrete profiles are subdivided into four different types. In the first type, different lithologies (but mainly yellow coloured sandstone layers) are capped by hard laminated crust (hardpan; Figure 4f) and in some cases, the uppermost part is made up by a pisolithic crust (Figure 4a). In the others a softpan horizon consists predominantly of nodules and a mixture of nodules and tubes, and also fracture-fill in red coloured mudstone (overbank deposits of an ancient meandering river) which grades up into hard laminated crust (Figure 4c–e). The second immature group of profiles is developed in the alluvial soil and includes calcrete powders, isolated nodules and tubes, and mixed nodule and tubes all of which rarely grade into laminar crust (Figures 4g, h & 5b). All calcrete profiles developed in near-surface settings and isolated calcrete horizons below the hard laminated crust in red mudstone (overbank deposits of the Kuzgun Formation) decrease in the direction of dip of the bed (Figure 4c). This is new and strong evidence to show that these calcretes were deposited from downward moving water. The thickness of the isolated horizons ranges from 0.5 to 2.5 m.

Petrography

Petrographic examination of thin-sections reveals that calcrete nodules, tubes and fracture fills are made up of predominantly dense micrite and also microsparite. Microsparite is a result of recrystallization because of etched boundaries with micritic areas.

Thin sections of hard laminated crust show that the samples are composed mainly of micrite and also microsparite. In thin sections, alpha and beta microfabric features are common (Figure 6). Alpha fabric is characterized by inorganic features such as wavy lamination, floating sediment grains, circumgranular cracking, clotted texture, fenestral pores, thin-crumbly fractures, vuggy pores, calcification of detrital grains (displacive replacement), and vadose silt. The wavy lamination is a characteristic feature of the hard laminated crust and consists of alternations of micrite, microsparite and rhizolitic mat laminae with thicknesses of 25 μm to 2 mm (Figure 6a). The sediment grains floating in micritic or pelletized matrix are predominantly monocrystalline quartz (Figure 6b) and also feldspar grains with an angular to subangular shape. They are 0.2 to 1 mm in size and are often surrounded by crystalline calcite or a dense micrite rim. Some quartz grains show a displacive replacement by calcite (see also Paquet & Ruellan 1997, p. 24–25). The circumgranular cracking is a minor diagenetic feature in the hardpan and is represented by spar-filled, crumbly fractures discontinuously surrounding grains (Figure 6c). The clotted texture is a common component of the alpha fabric in the hard laminated crust and is composed of micritic grains of ellipsoidal or spherical shape with size of 30–150 μm. The peloids are predominantly 30–70 μm in size. The peloids are separated from each other by polygonal or wedge-shaped microfractures filled by microspar. Fenestrae are elongate pores having a long axis 0.1 to 2.2 mm in length; they are partly or completely filled by calcite microspar or spar. Fenestral pores are often associated with clotted texture or wavy lamination. Thin-crumbly fractures are non-tectonic fractures filled by calcite microspar and are often associated with clotted texture and microbreccia consisting of microscopic size intraclast and peloids. Vuggy pores are scarce and filled by calcite

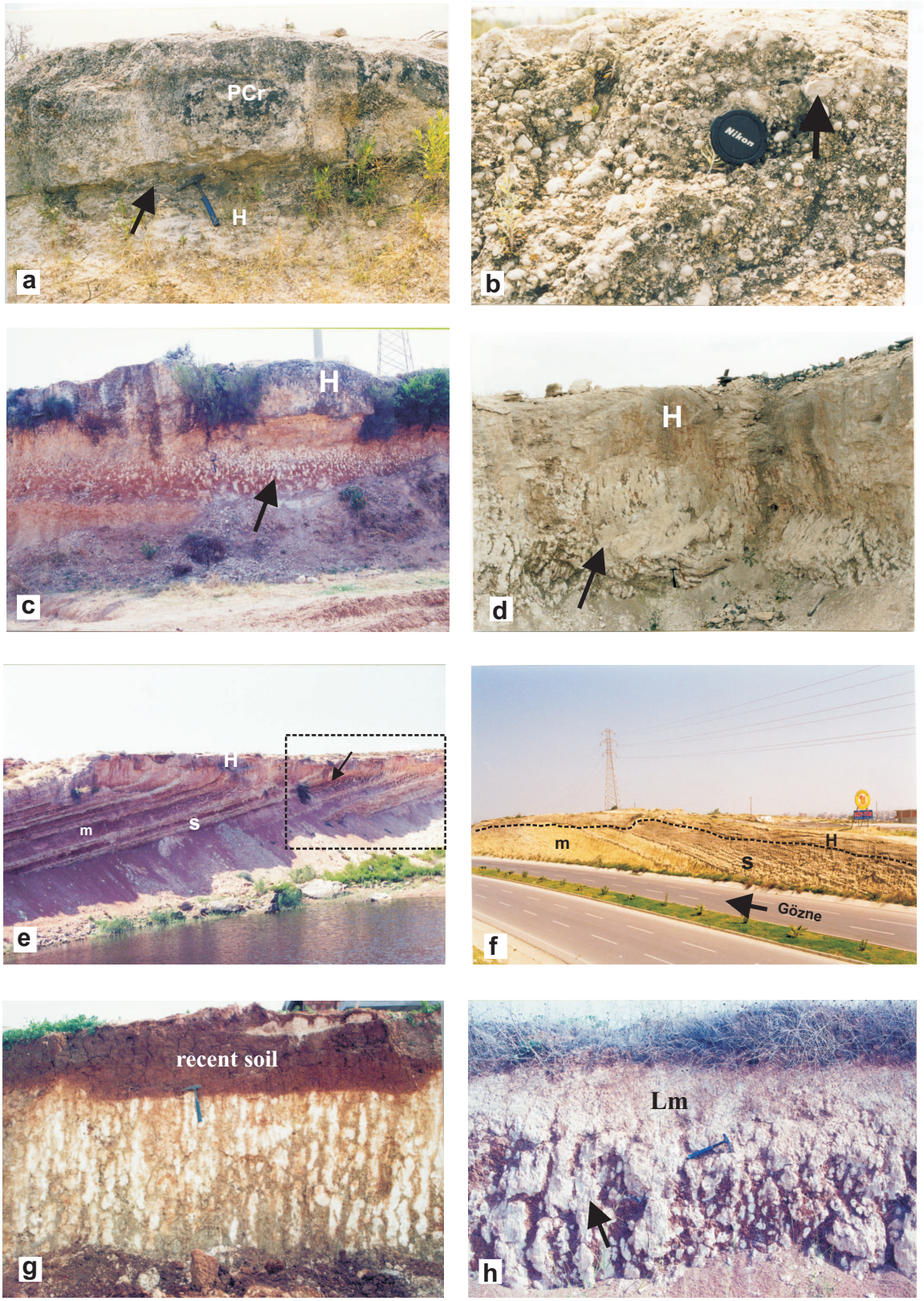

Figure 4.

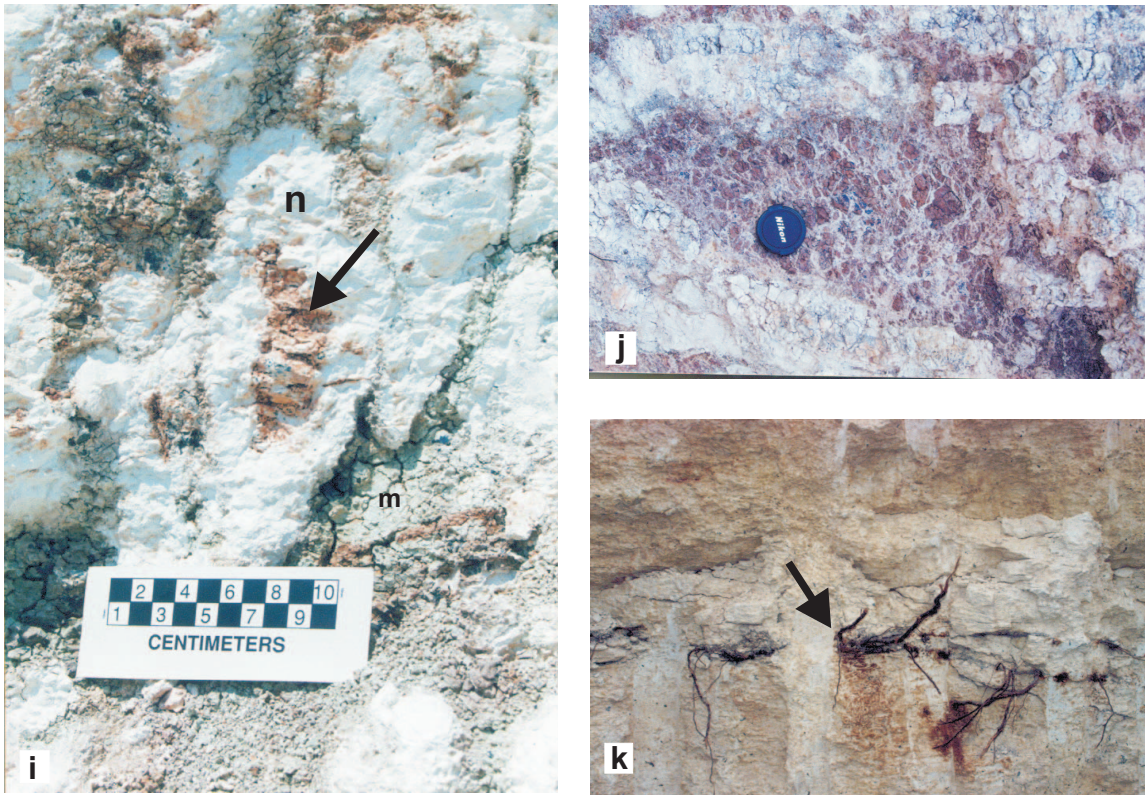

Figure 4. Field photographs showing calcrete occurrences in and/or over the Kuzgun Formation (Tortonian, Miocene) and in alluvial red soil (Quaternary): **(a)** pisolithic crust (PCr) overlying the hard laminated crust (H) with an erosional surface (arrow); **(b)** close-up of the pisolithic crust showing poorly sorted pisolithes (arrow); **(c)** the hard laminated crust (H) capping the nodular calcrete horizon (arrow) in red coloured mudstone of the Kuzgun Formation; **(d)** the hard laminated crust (H) overlying the nodular and tubular horizon (arrow) in the mudstone (the Kuzgun Formation). The transition is gradual from hard laminated crust to nodular and tubular horizon; **(e)** the hard laminated crust (H) capping alternating beds of the ancient meandering river deposits of the Kuzgun Formation. Nodular and tubular calcretes (arrow in frame) appear in near-surface parts of red-coloured mudstone beds (m) and decrease in down-dip direction. (s) indicates a sandstone bed; **(f)** the hard laminated crust (H) capping yellow coloured mudstone (m) and sandstone (s) beds of the Kuzgun Formation; **(g)** calcrete nodules and tubes (white mottlings) in the alluvial red soil below the recent soil cover. The calcrete occurrence caused colour change in the soil from red to green; **(h)** calcrete horizon in the alluvial red soil below the vegetation showing laminated crust (Lm) grading into nodular and tubular horizon (arrow); **(i)** Calcrete nodule (n) showing relics of red mudstone (m) of the Kuzgun Formation at the centre (arrow); **(j)** honeycomb-like structure below the hard laminated crust in which calcrete fills thin non-tectonic fractures in red-coloured mudstone (the Kuzgun Formation) and indicates a gradational transition from the hard laminated crust to host-rock; **(k)** root-mat (arrow) within the hard laminated crust.

spar or microspar and associated with a microbreccia texture. Vadose silt is composed of detrital calcite with a 10–50 μm size and occurs within interstitial pores and rhizo-molds.

Beta fabric originated by biogenic activity and is represented by rhizoliths (root petrification, root mould, root cast), alveolar septal fabric, calcite needles, spherulite-like structures, and vadose (calcrete) pisoliths. Rhizoliths are organo-sedimentary structures produced by petrification of roots (Klappa 1980). Their equatorial sections are irregularly circular or elliptical in shape and longitudinal sections appear as irregular tubes, in some cases showing bifurcation. Equatorial sections often show cellular cortex structures (Figure 6d). The root-walls are made up predominantly of dense micrite and rarely of calcite needles. The root-voids are produced by the decay of the central part of roots and are generally filled by sparry calcite and rarely by calcite needles; some are empty. Root-casts are formed by irregular root-molds filled by sparry calcite or vadose silt. Alveolar texture (Figure 6d) is represented by a complex network of cylindrical to irregular root-voids surrounded by micrite or a bundle of

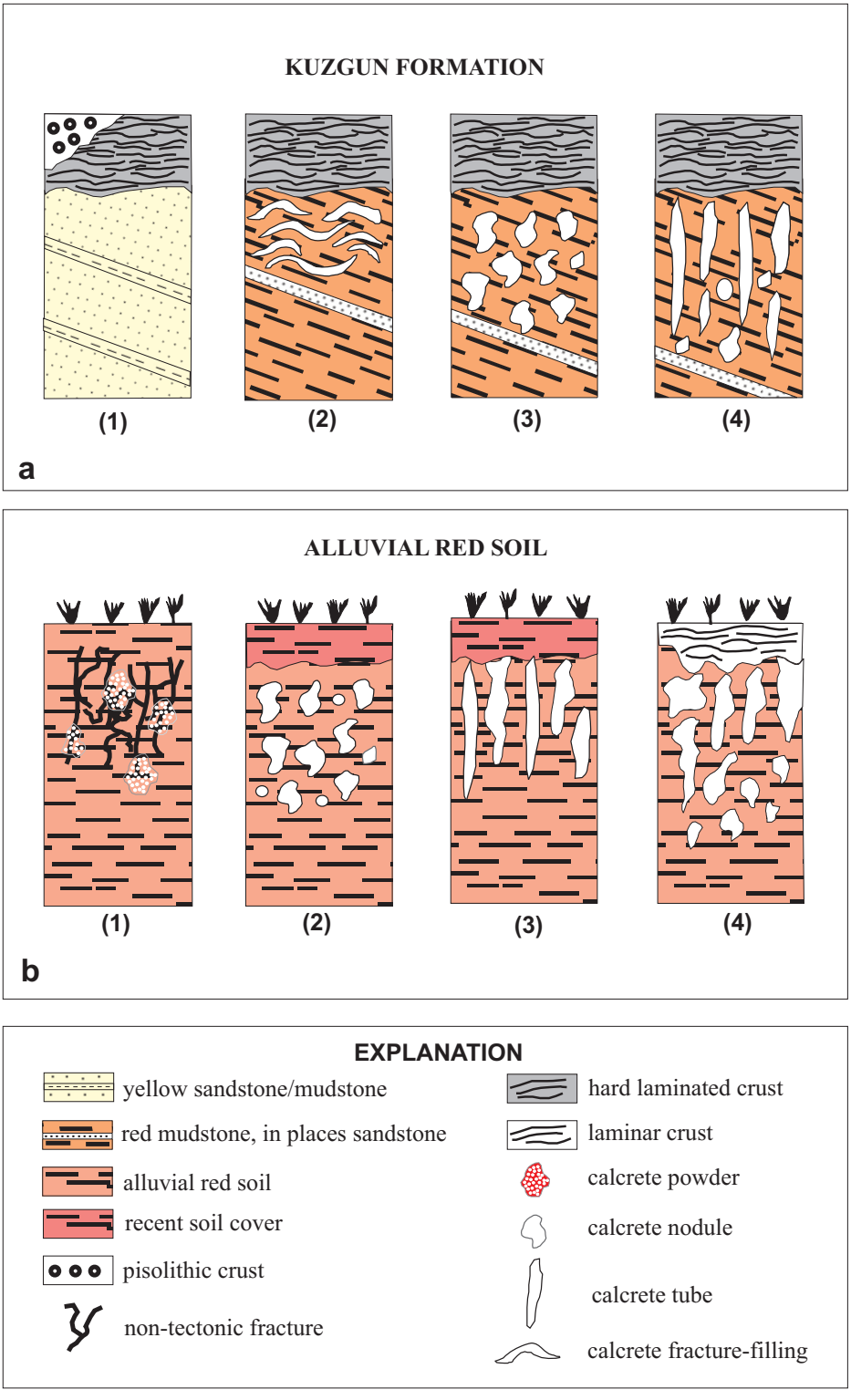

Figure 5. Schematic presentation of calcrete profiles (a) in and/or over the Kuzgun Formation and (b) in the alluvial red soil.

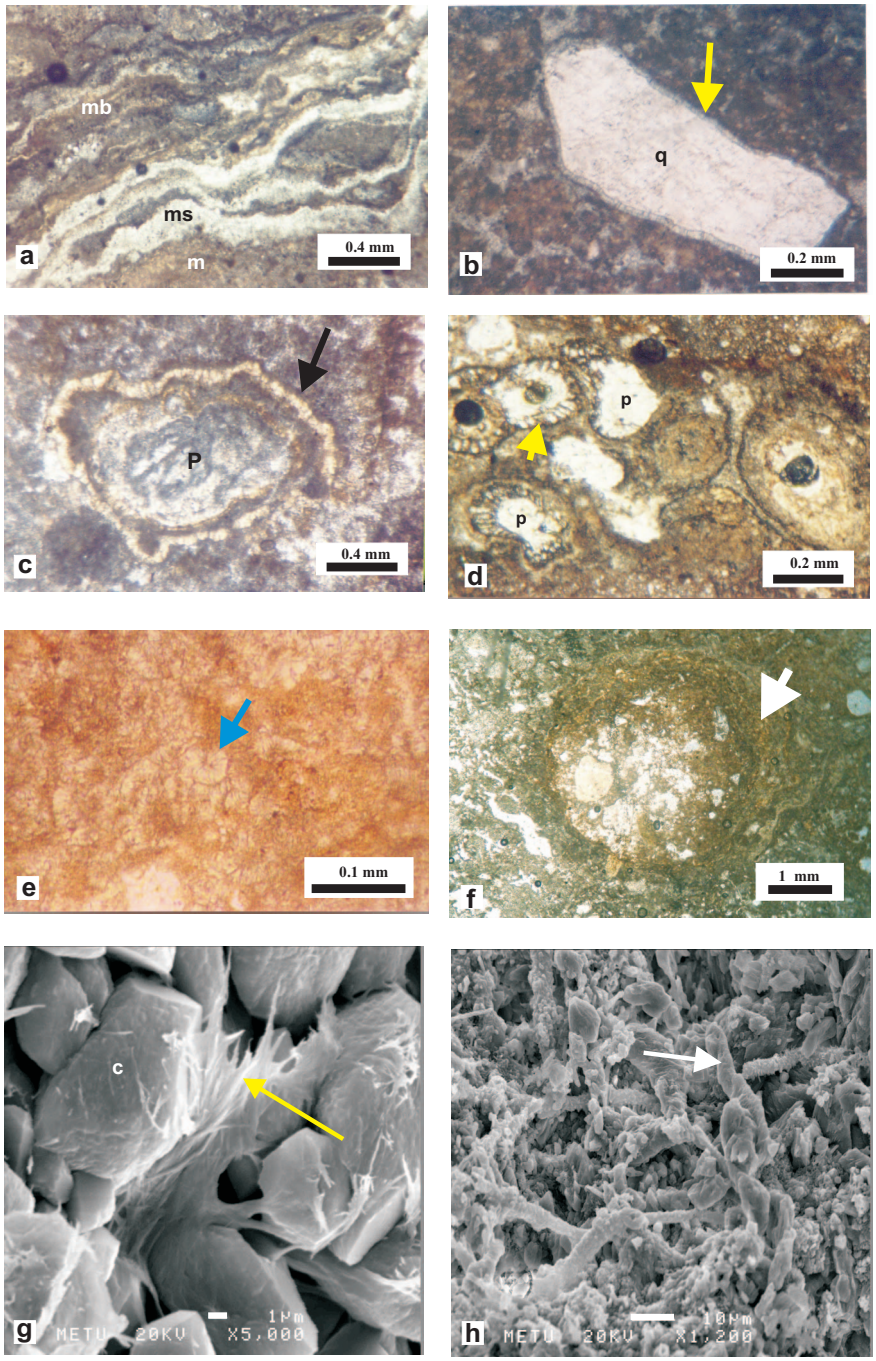

Figure 6. Micromorphological features of the calcretes: **(a)** lamination in the hard laminated crust consisting of wavy micrite (m), microsparite/sparite (ms), and microbial (mb) laminae; **(b)** floating quartz grain (q) with microsparitic rim (arrow) in the pelletized micritic matrix. Hard laminated crust; **(c)** circumgranular crack with sparry calcite infill (arrow) surrounding calcrete pisolith (p). Hard laminated crust; **(d)** rhizoliths (root–petrifaction) with cellular cortex structure (arrow) in an alveolar texture. p: pore; hard laminated crust; **(e)** Spherulite-like microcodium (arrow) consisting of radiating calcite prisms. Hard laminated crust; **(f)** calcrete (vadose) pisolith (arrow) showing poorly laminated, microbial coatings and downward growing (pendant; right side). Hard laminated crust; **(g)** SEM view of calcrete nodule consisting of euhedral to subhedral calcite crystals (c) from which fibre bundles of palygorskite (arrow) extend; **(h)** SEM image showing an irregular network of calcified filaments.

parallel to subparallel oriented calcite needles (Esteban 1974; James & Choquette 1984; Goudie 1996); calcified fungi are also associated with rhizocretions (Wright *et al*. 1988; Tucker & Wright 1990; Jimenez de Cisneros *et al*. 1993). Calcite needles are also seen in interstitial spaces of rhizoliths forming a mesh-like structure and also in root-voids as randomly oriented needles. Spherulite-like structures are observed in some thin-sections (Figure 6e). They are circular or elliptical in shape with a size of 20–70 μm, exhibiting radial-fibrous calcite crystals radiating from a central cavity (Flugel 2004). These structures are considered to be the neomorphosed form of *Microcodium* (Rao 1990), which is of microbial origin (Klappa 1978). Calcrete (vadose) pisoliths are composed of irregularly coated microbial laminae around a nucleus showing a downward elongation that indicates an in-situ formation (Figure 6f) (Hay & Reeder 1978). Their size varies from 0.3 to 3 mm. The coatings are produced by microbial calcification (Calvet 1982; Calvet & Julia 1983; Tucker 1991).

Scanning Electron Microscopy (SEM-EDX) Analysis

SEM images show that calcrete nodules, tubes and pisoliths are predominantly composed of equigranular mosaics of calcite crystals (Figure 6g) with size of less than 10 μm and xenotopic to hypidiotopic textures. Intercrystalline micropores are present, and some calcite crystals show etched boundaries due to partial leaching. In the samples, palygorskite clay minerals often appear as a minor diagenetic constituent, and smectite flakes are rarely present as a relic of host-rock or sediment. Palygorskite occurs in the forms of fibres and fibre bundles (Figure 6g) 0.5 to 3 μm in length on the calcite crystals and also with smectite flakes growing into the pore-spaces among the crystals.

SEM views of hard laminated-crust often show an irregular network of calcified filaments (Figure 6h), sometimes associated with calcite needles and spherical calcite bodies. The filaments are straight to curved in shape, and some show small internal tubes, surrounded by an irregular coat of microcrystalline calcite. The filaments are 3–5 μm in diameter and up to 90 μm in length; their walls consist of micrite-sized calcite crystals. On some filaments isolated spherical calcite bodies with diameters up to 5 μm are present. The calcite needles are randomly oriented and perpendicular to the calcified filaments. They appear in lath shapes with smooth surfaces, and are up to 10 μm long and 0.5 to 1 μm wide. The calcified filaments and associated calcite needles are interpreted as the result of fungal biomineralization (Wright 1986; Jimenez de Cisneros *et al*. 1993; Verrecchia *et al*. 1993; Jimenez-Espinosa & Jimenez- Millan 2003; Bajnoczi & Kovacs-Kis 2006). However, Phillips *et al*. (1987) suggest that four main groups of micro-organisms such as fungi, algae, bacteria and lichens have filamentous structures that may be precursors to the calcified filaments. A root-hair origin is also proposed for some branching calcified filaments (Ward 1975; Klappa 1979, 1980). Similar to calcified filaments, a variety of origins have been proposed to explain the occurrence of calcite-needles. These are: (1) precipitation from an extremely supersaturated evaporative solution in near surface environments, and (2) a biogenic or microbial origin especially of fungi and root-hair (Wright & Tucker 1991; Goudie 1996). Verrecchia *et al.* (1993) suggested that calcite needles associated with fungal filaments are calcium oxalate. The spherical calcite bodies are attributed to fungal spores or bacteria (Jones & Ng 1988; fungal spore, Nash & McLaren 2003; bacteria, Alonso-Zarza & Arenas 2004).

SEM analyses of host-rocks, which are red coloured mudstone of the Kuzgun Formation often associated with calcrete nodules and tubes, reveal that the mudstone consists of smectite flakes possibly of detrital origin. In the mudstone sample taken close to the calcrete occurrence, in this case the sample shows palygorskite fibres and fibre bundles similar to calcrete samples. They originated either from water by precipitation or by transformation of smectite flakes.

Mineralogy and Geochemistry

XRD Analysis. X-ray diffraction analysis was used to determine the mineralogical composition of calcrete samples and their host-rocks and sediments and semi-quantitative mineral abundance in the samples. The results are shown in Table 1. The calcrete samples consist mainly of calcite associated with minor smectite and palygorskite and accessory quartz, feldspar, illite and dolomite. The smectite is the remains of the host-rock or sediment, and its abundance in the samples is due to the degree of calcification and sampling.

XRD analysis reveals that smectite is a dominant clay mineral in the red coloured mudstones (overbank deposits of the Kuzgun Formation) and red alluvial soils in which

Table 1. Semi-quantitative analyses obtained by X-ray diffraction of selected samples.

sample no	calcite	dolomite	quartz	feldspar	illite	palygorskite	smectite
mudstone (the Kuzgun Formation) / alluvial red soil (clay)*							
K-1	+		+	ac		++	++
K-2	+		+			++	++
K-3	+		+	ac	ac	++	++
K-4	+		ac	ac	+		++++
K-5	+		ac	ac	ac	+	+++
K-5B	ac		ac	ac	+	+	+++
K-5C	+		ac	ac	+	ac	++++
K-6	ac		ac	ac	ac	ac	++++
K-7	ac		ac	ac	+	+	+++
K-8			ac	+	+		+++
K-9	+		+	ac	ac	+	+++
K-9B*	+		ac		+		+++
K-10			ac	ac	ac	++	+++
K-11			ac	ac	+	ac	++++
K-12	+		+	+	ac	+	+++
ZU-1*	+		+	ac	ac	ac	++++
E-9	+		ac	ac	ac	+	+++
E-14	+		ac	ac	ac	+	+++
E-16	+		ac	ac	ac	+	+++
E-25	+		ac	ac	ac	+	+++
E-26	+		ac	ac	ac	+	+++
E-33	+		ac	ac	ac	+	+++
E-62*	+		+	ac	ac	+	++
E-30	+		ac	ac	ac	+	+++
calcrete nodule, tube* and fracture-fill**							
E-8	++		ac	ac	+		++
E-15	+++		ac	ac	ac		++
E-17*	++		ac	ac	+		++
E-18*	++++		ac				+
E-20	+++		ac		+		+
E-22**	+++		ac			+	+
E-23**	+++		ac			+	+
E-24**	+++		ac		ac	+	+
E-28	+++		ac		+		+
E-29	+++		ac		+		+
E-31	+++		ac			+	+
E-32	++++					+	
E-60	++++		ac		+		+
E-61*	+++		ac		+	ac	+
E-64	+++		ac		+	+	ac
E-2*	++++		+	ac		ac	ac
K-2*	++++					ac	+
C-1*	++++					ac	ac

+ : relative abundance of minerals; ac : accessory

Table 1. (Continued)

sample no	calcite	dolomite	quartz	feldspar	illite	palygorskite	smectite
			calcrete nodule, tube* and fracture-fill**				
G-1*	+++		ac			ac	+
1-A	+++		ac			+	+
1-B	++++						+
2-A	++++		ac			+	
2-B	++++		ac			+	ac
3	+++		ac			+	+
4	+++		ac			ac	++
5	+++		ac		ac		++
6-A	++++						+
6-B	++++		ac			ac	+
7-A	++++						+
7-B	++++						+
8	+++		ac				++
9	++++		ac				+
10	+++		ac			+	+
11-A	+++		ac	+			+
11-B	+++++						
12	+++++						
			hard laminated crust (hardpan)				
H-1	+++	+	ac				+
H-2	+++		+				+
H-3	+++		+			ac	+
H-4	++++		ac				+
H-4	++++		+	+			
H-5	+++++	ac	ac				
H-6	++++		+				+
H-8	+++++		ac				
H-9	++++		ac			ac	+
HP-1	+++		+	+			+
HP-2	+++		+				+
HP-3	+++		+	ac			+
HP-4	+++		+	+			+
HP-5	+++		+	+	ac		+
HP-6	+++		+	+		ac	+
HP-7	++++		+				ac
HP-8	++++		+			ac	
HP-9	+++		+			ac	+
HP-11	+++		+	+			+
HP-12	+++		+	ac			+
HP-13	++++		+				ac

calcrete formation is common. In the samples, smectite is associated with small amounts of calcite and palygorskite related to calcrete formation and also with accessory quartz, feldspar and illite.

ICP-AES Analysis. ICP-AES analyses were performed on the calcrete samples and their host-rocks or sediments to determine their chemical composition. The results are represented in Table 2. All calcrete samples demonstrate high CaO values, variable SiO_2 and Al_2O_3 contents and low Sr-content similar to the parent material, except pisolithic crust samples which have relatively high Sr values of 834 to1255 ppm. Sr enrichment in pisoliths probably reflects relatively more Ca supply from marine carbonates in the local area. The results of the parent materials are typical for siliceous mudstones and clay-rich sediments. These samples contain variable CaO values as a function of calcite replacement and Fe_2O_3 values of 2.65–6.60 wt%. These Fe_2O_3 values are typical for red sedimentary-rocks or unconsolidated sediments (Van Houten 1973; Eren & Kadir 1999). Trace element (Ba, Cu, Zn, Ni, Co, Zr, Ce, Y, Nb, Sc) concentrations in the calcretes have been inherited from the host-rocks and sediments with varying depletion due to their removal by infiltrating water.

Stable Isotopes. Stable isotope values of calcrete samples are listed in Table 3 and plotted in Figure 7. The crossplot (Figure 7) shows $\delta^{18}O$ and $\delta^{13}C$ values of distinctive calcrete groups and present-day groundwater. There is an inverse covariation between $\delta^{18}O$ and $\delta^{13}C$ values. The calcite $\delta^{18}O$ and $\delta^{13}C$ values of calcretes range from –4.31 to –6.82 and from –6.03 to –9.65 ‰ PDB, respectively. The oxygen isotope values exhibit a very narrow range, whereas carbon isotope values have a somewhat larger range (Figure 7). The oxygen isotope values are typical for calcretes, reflecting formation under the influence of meteoric water (James & Choquette 1984; Purvis & Wright 1991; Strong *et al*. 1992; Jimenez de Cisneros *et al*. 1993; Shaaban 2004; Gong *et al*. 2005). In the study area, present-day groundwater has $\delta^{18}O$ values ranging from –5.9 to –8.4 with a mean value of –7.12 ‰ V-SMOW (Hatipoğlu 2004). $\delta^{18}O$ enrichment in calcretes with respect to present-day groundwater is due to evaporative removal of light isotopes from water (Gong *et al*. 2005). The negative calcite $\delta^{13}C$ values of calcretes clearly indicate a high input of soil-zone carbon presumably derived from the decay of C_3 organic matter (Goudie 1983; Cerling 1984; Purvis and Wright 1991; Lee 1999; Tandon & Andrews 2001; Robinson *et al*. 2002; Alonso-Zarza & Arenas 2004). The pisolithic crust samples have relatively heavier or less negative calcite ^{13}C values in respect to the other samples (Figure 7). The difference in calcite $\delta^{13}C$ values can be explained by variable contributions of atmospheric CO_2 and soil-derived CO_2 (Cerling 1984). The less negative calcite $\delta^{13}C$ values of pisolithic crust samples showing enrichment in ^{13}C indicate a formation from surface-water relatively less influenced by soil CO_2 or due to kinetic isotope effects associated with evaporation (Knauth *et al*. 2003).

Interpretation and Discussion

Age and Climatic Change

Calcrete formation in Turkey is related to climatic changes during Pleistocene to Early Holocene times. This is based on field observations (Atalay 1996; Kapur *et al*. 1987, 1990, 2000) and ESR and TL dating methods which date calcretes from 250 to 782 ka BP in the Adana region (Özer *et al*. 1989; Atalay 1996). In the Mersin area, calcretization took place at the same time with few interruptions, and affected exposed argillaceous rocks of the Kuzgun Formation (Tortonian), and alluvial red soils (Quaternary). As mentioned earlier, calcretes form under a wide range of rainfall from 200 to 600 mm/year. The presence of palygorskite in the calcretes (see also Kapur *et al*. 1987) is indicative of semi-arid or seasonally arid (<300 mm/year) climatic conditions (Sancho *et al*. 1992) suggesting a climatic change from Pleistocene–Early Holocene to Recent. Present day climatic conditions with annual precipitation of 634 mm reflect more humid climatic conditions compared to Pleistocene–Early Holocene times. This climatic change is also supported by small-scale karstic features (karren) on the hard laminated crust and there is no clear evidence to indicate present-day calcretization.

Evolution and Origin

In the study area, the analyses show that calcrete samples consist predominantly of calcite with palygorskite present in the samples as a minor component. In this region calcretes are commonly observed at topographic heights of 20 to 250 m and the various calcrete forms appear in near surface settings of small ridges and highs with

Table 2. Chemical analyses of selected calcrete and host-rock/sediment samples.

sample no	SiO_2 %	Al_2O_3 %	Fe_2O_3 %	MgO %	CaO %	Na_2O %	K_2O %	TiO_2 %	P_2O_5 %	MnO %	Cr_2O_3 %	Ba ppm	Cu ppm	Zn ppm	Ni ppm	Co ppm	Sr ppm	Zr ppm	Ce ppm	Y ppm	Nb ppm	Sc ppm	LOI %	SUM %
red mudstone (the Kuzgun Formation) / alluvial red soil (clay*)																								
K-1	42.25	9.00	5.21	3.14	14.28	.11	1.66	.45	.03	.08	.034	141	39	37	172	24	164	54	41	10	<10	13	23.7	100.03
K-2	41.15	6.60	3.04	2.40	20.18	.30	.90	.35	.02	.07	.047	141	22	<20	124	<20	282	64	26	<10	12	8	24.8	99.94
K-3	39.64	9.47	5.68	3.51	14.42	.15	.86	.52	.06	.08	.026	83	46	34	195	25	185	61	40	10	<10	15	25.4	99.91
K-4	43.82	11.68	6.30	3.09	10.10	.19	1.06	.60	.05	.09	.023	166	44	53	192	26	184	77	65	10	<10	16	22.9	100.01
K-5	42.46	11.19	6.61	3.41	10.61	.14	1.60	.57	.05	.08	.030	148	37	53	238	26	170	64	30	10	<10	17	23.1	99.95
K-5B	48.57	12.13	6.57	3.08	5.26	.24	1.29	.61	.02	.03	.031	120	40	44	168	<20	79	73	<20	<10	<10	17	22.1	100.00
K-5C	40.70	10.29	5.86	2.79	13.06	.23	1.20	.51	.04	.07	.023	125	39	139	215	35	153	62	42	<10	<10	14	25.2	100.08
K-6	47.67	12.02	6.48	3.20	6.01	.24	1.16	.60	.02	.08	.032	131	32	53	219	24	83	86	64	<10	21	16	22.4	100.01
K-7	48.27	12.09	6.07	3.46	5.02	.20	1.69	.58	<.01	.04	.030	128	31	56	199	30	52	82	36	<10	<10	15	22.5	100.03
K-8	53.35	13.71	2.65	4.22	2.66	.29	0.56	.30	<.01	.02	.020	94	30	<20	46	<20	58	105	71	<10	<10	6	22.2	100.03
K-9	43.93	11.34	5.50	1.46	12.76	.17	1.43	.61	.01	.07	.054	194	30	50	145	22	88	129	61	13	12	13	22.6	100.03
K-9B*	46.71	12.26	6.07	1.45	10.25	.26	1.60	.69	.01	.08	.062	188	25	53	195	22	67	144	81	14	10	15	20.5	100.04
K-10	51.92	14.15	6.24	3.48	1.47	.19	2.45	.69	<.01	.03	.045	171	39	55	86	<20	48	117	24	<10	<10	17	19.3	100.03
K-11	50.25	14.12	5.83	2.93	3.46	.12	1.49	.58	.01	.02	.033	109	45	58	76	<20	45	96	47	<10	10	16	21.1	100.01
K-12	44.86	10.19	5.38	2.90	11.76	1.21	1.55	.58	.08	.06	.048	226	24	45	190	24	256	105	61	14	<10	13	19.3	100.04
ZU-1*	45.80	10.77	5.06	1.77	12.55	.14	1.20	.69	.03	.10	.055	438	22	46	136	21	109	157	80	21	19	12	22.0	99.99
hard laminated crust																								
N-1	1.02	.05	.04	.35	54.17	<.01	<.02	<.01	.02	<.01	.002	67	<20	<20	<20	<20	150	<10	<20	<10	<10	<1	44.2	99.88
N-3	15.44	.59	.30	.70	44.34	.03	.07	.03	.01	<.01	.003	107	<20	<20	<20	<20	202	<10	<20	<10	<10	1	38.4	99.97
N-5	7.84	.87	.28	.32	49.56	.08	.17	.04	<.01	.01	.010	63	<20	<20	<20	<20	125	15	<20	<10	<10	1	40.7	99.91
N-8	2.82	.70	.39	.36	52.30	.03	.06	.03	<.01	.01	.004	36	<20	<20	22	<20	75	<10	<20	<10	<10	1	43.2	99.93
N-10	5.36	.89	.39	.50	50.74	.08	.15	.04	<.01	.01	.009	62	<20	<20	38	<20	260	<10	<20	<10	<10	1	41.8	100.02
H-1	1.72	.49	.26	.29	53.35	<.01	.06	.02	<.01	<.01	.002	34	<20	<20	<20	<20	121	<10	<20	<10	<10	1	43.7	99.93
H-3	3.62	.59	.26	.33	52.17	.03	.13	.03	<.01	<.01	.006	47	<20	<20	<20	<20	121	<10	<20	<10	<10	1	42.8	99.99
H-4	5.16	.80	.33	.39	50.89	.08	.19	.04	.02	<.01	.008	65	<20	<20	<20	<20	141	20	<20	<10	<10	1	42.1	100.04
H-5	3.50	.58	.24	.28	52.18	.04	.13	.03	.01	<.01	.004	53	<20	<20	<20	<20	95	<10	<20	<10	<10	1	42.9	99.92
H-8	1.03	.24	.12	.32	54.22	.02	.04	<.01	<.01	<.01	.001	53	<20	<20	<20	<20	128	20	<20	<10	<10	<1	43.9	99.93
H-9	3.01	.77	.39	.39	52.10	.02	.11	.04	<.01	.01	.003	58	<20	<20	<20	<20	110	<10	<20	<10	<10	1	43.1	99.97
E-4	7.06	.77	.19	.34	50.09	.07	.22	.03	<.01	<.01	.007	72	<20	<20	<20	<20	194	10	<20	<10	<10	<1	41.2	100.02
E-13	10.21	.86	.18	.35	48.42	.12	.28	.05	<.01	.01	.027	125	<20	<20	<20	<20	174	37	<20	<10	<10	<1	39.5	100.05
E-66	**10.40**	**.59**	**.17**	**.37**	**48.72**	**.03**	**.13**	**.02**	**<.01**	**.01**	**.006**	**78**	**<20**	**<20**	**<20**	**<20**	**163**	**<10**	**<20**	**<10**	**<10**	**<1**	**39.6**	100.07
calcrete nodule and tube (*)																								
A-1	7.81	1.44	.69	.55	48.92	.02	.25	.07	.01	.01	.008	26	<20	<20	20	<20	64	<10	<20	<10	<10	1	40.2	100.00
K-3*	2.85	.45	.25	.45	52.51	.01	.05	.02	<.01	<.01	.003	20	<20	<20	<20	<20	135	<10	<20	<10	<10	<1	43.4	100.03
G-1*	2.86	.59	.32	.42	52.69	<.01	.07	.03	<.01	<.01	.003	22	<20	<20	<20	<20	83	<10	<20	<10	<10	1	43.0	100.01
K-1*	2.83	.65	.31	.53	52.08	.02	.06	.03	.01	<.01	.003	25	<20	<20	<20	<20	143	<10	<20	<10	<10	1	43.5	100.05
8	5.19	1.26	.26	.64	50.84	.04	.07	.03	<.01	<.01	.004	15	<20	<20	<20	<20	77	13	<20	<10	<10	<1	41.7	100.05
1-A	11.43	2.54	1.35	1.00	44.56	.04	.35	.12	<.01	.02	.012	39	<20	<20	49	<20	101	22	<20	<10	26	3	38.5	99.97
B-3	7.01	1.04	.34	.43	50.21	.07	.23	.04	<.01	.01	.004	58	<20	<20	<20	<20	67	<10	<20	14	<10	1	40.6	100.00
2-B	3.17	.50	.28	.50	52.56	<.01	.04	.03	<.01	.01	.003	11	<20	<20	<20	<20	123	<10	<20	<10	<10	<1	42.9	100.00
3	8.04	1.85	1.09	.92	47.32	.03	.17	.10	.02	.02	.006	21	<20	<20	29	<20	132	<10	<20	14	13	3	40.4	99.99
G-3*	1.06	.23	.12	.32	54.85	<.01	.02	<.01	<.01	<.01	.001	10	<20	<20	<20	<20	70	<10	<20	<10	<10	<1	43.4	100.02
A-3	8.84	1.65	.79	.59	47.88	.03	.31	.08	<.01	.02	.008	35	<20	<20	26	<20	73	<10	<20	<10	<10	2	39.9	100.11
B-1	3.06	.75	.43	.38	52.41	.04	.08	.04	<.01	.01	.003	18	<20	<20	<20	<20	47	<10	<20	15	<10	1	42.8	100.01
6-A	5.48	1.37	.78	.67	49.72	.02	.11	.07	<.01	.01	.003	19	<20	<20	26	<20	158	<10	<20	<10	10	1	41.7	99.97
10	5.65	1.33	.55	.46	50.36	.03	.22	.06	<.01	.02	.004	19	<20	<20	<20	<20	54	<10	<20	11	<10	1	41.4	100.10
9*	9.07	2.43	1.23	.52	46.89	.04	.30	.14	<.01	.02	.008	43	<20	<20	38	<20	50	22	<20	<10	12	3	39.4	100.08
4	2.61	.49	.27	.39	52.45	<.01	.04	.02	<.01	<.01	.002	14	<20	<20	<20	<20	85	<10	<20	<10	<10	<1	43.6	99.90
2-A	5.73	.84	.46	.70	50.68	.03	.08	.04	<.01	.01	.002	13	<20	<20	<20	<20	158	<10	<20	<10	<10	1	41.4	100.00
11-B	1.10	.31	.12	.25	54.71	.02	.03	.01	<.01	<.01	.003	14	<20	<20	<20	<20	50	<10	<20	<10	<10	<1	43.4	99.97
7-A	3.57	.96	.51	.47	52.10	<.01	.06	.04	<.01	<.01	.004	18	<20	<20	<20	<20	111	<10	<20	<10	<10	1	42.2	99.95
5	6.10	1.12	.56	.56	50.08	.03	.08	.05	<.01	.01	.002	14	<20	<20	<20	<20	145	<10	<20	<10	<10	1	41.4	100.02
pisolithic crust																								
Piz-7	2.90	.52	.36	.82	51.14	.01	.07	.03	.01	.04	.009	44	<20	<20	30	<20	875	<10	<20	<10	<10	1	44.0	100.03
Piz-8	.55	.08	.42	.93	53.46	.04	<.02	<.01	.01	.04	.002	44	<20	<20	<20	<20	1255	<10	<20	<10	<10	1	44.2	99.90
Piz-9	.92	.14	.32	.74	53.32	.01	.03	<.01	.02	.02	.001	41	<20	<20	<20	<20	834	<10	<20	<10	<10	1	44.3	99.94
Piz10	.79	.15	.48	.84	53.28	<.01	.02	<.01	.02	.02	.003	50	<20	<20	23	<20	934	<10	<20	<10	<10	1	44.2	99.93
Piz11	.93	.18	.39	.82	53.37	<.01	.02	<.01	.01	.01	.002	47	<20	<20	<20	<20	851	<10	<20	<10	<10	1	44.1	99.96
Piz12	**.72**	**.14**	**.42**	**.82**	**53.54**	**.03**	**.02**	**<.01**	**.02**	**.01**	**.001**	**45**	**<20**	**<20**	**<20**	**<20**	**840**	**<10**	**<20**	**<10**	**<10**	**1**	**44.1**	99.93

* Analyzed by ICP-AES; LOI: loss on ignition

Table 3. Stable isotope data of selected calcrete-calcite samples.

sample	$\delta^{18}O$	$\delta^{13}C$
hard laminated crust		
H-1	-5.26	-9
H-3	-4.92	-8.89
H-4	-4.89	-8.66
H-5	-4.97	-9.03
H-8	-5.25	-9.07
H-9	-5.25	-8.9
E-4	-5.47	-8.49
E-13	-5.84	-8.91
E-66	-5.31	-8.56
nodule, tube* and fracture-fill**		
7-A	-5.13	-8.7
11-B	-5.39	-8.79
0-2*	-5.07	-8.61
E-23**	-5	-8.54
K-1**	-5.18	-8.74
E-18*	-5.58	-8.63
E-32	-5.59	-8.4
12	-5.43	-8.66
E-60	-4.31	-9.65
2-B	-4.56	-8.43
pisolith		
Piz-8	-5.91	-6.25
Piz-9	-6.6	-6.58
Piz-10	-6.65	-6.2
Piz-11	-6.53	-6.03
Piz-12	-6.82	-6.34

powdery to indurated crusts. In the field, several calcrete profiles have been described and mainly subdivided into two major groups comprising mature and immature profiles. Their formation shows three distinct stages of calcrete development.

The early stage is characterized by a mottled or plugged horizon including isolated calcite accumulations such as powdery, nodule, tube and fracture-filling. They were formed as a result of precipitation of predominantly calcium carbonate and also palygorskite from downward percolating meteoric water (Gile *et al*. 1966; Knox 1977; Watts 1980; Arakel 1982) and/or replacement of host-rock or sediments by calcite (Watts 1980; Wang *et al*. 1994) and also palygorskite in the vadose zone (Wall *et al*. 1975). The mottled horizon is developed below the zone of biological activity and samples exhibit alpha fabrics comprising mostly dense micrite. The vadose origin is based on the near-surface settings of this type of calcrete and their decrease downward into the host beds. The red mudstones (floodplain deposits) of the Kuzgun Formation and alluvial red soils are more favourable for the growth of isolated calcrete forms due to their selective occurrence. Intense fracturing in the red mudstones breaking the rock into cubic or prismatic blocks of various sizes and irregular desiccation cracks in the red alluvial soil played an important role in the development of some calcrete forms such as nodule, tube and fold-like shapes and also in the downward transportation of surface waters. The erosional surface cross-cutting early formed calcretes in red mudstone of the Kuzgun Formation indicates an interruption in calcrete development caused by the climatic fluctuation (Atalay 1996). Figure 8 shows the simplified pattern of calcrete development. The calcite $\delta^{18}O$ and $\delta^{13}C$ values reflect meteoric water conditions and an input of light CO_2 derived from soil-zone, respectively. The dense micritic calcite suggests relatively rapid precipitation (Tucker & Wright 1990; Wright & Tucker 1991; Nash & McLaren 2003) from evaporated soil-derived water. The palygorskite also precipitated from the same water at an advanced stage of evaporation as evidenced by the presence of palygorskite fibres and fibre bundles extending from fine calcite crystals (Watts 1980).

The second stage is characterized by calcareous crusts comprising hard laminated crust (hardpan calcrete) and laminar crust. The laminar crust is interpretated as an initial stage of hard laminated crust. The hard laminated crust is widespread and easily recognizable in the field; it appears to vary little in appearance. Hence more data are provided for the hard laminated crust. The planar calcrete forms have developed over the plugged horizon characterized by early stage calcrete forms (Gile *et al*. 1966; Reeves 1970; Read 1974; Arakel 1982; Arakel & McConchie 1982; Wright *et al*. 1988, 1995; Rossinsky & Wanless 1992). The plugged horizon drastically reduced the downward movement of percolating soil-water and caused lateral movement of soil-water in the vadose zone; this is evidenced by calcrete pisoliths, vadose calcite silts, alveolar texture, calcite needles and desiccation fractures (circumgranular cracks and crumbly fractures). The lateral movement of percolating water has resulted in lamination which consists of alternating laminae of predominantly micrite and rhizolitic-microbial mat, indicating repeated conditions of dry and wet periods due to seasonal variations (Gile *et al*. 1981; Lal & Kimble 2000; Candy *et al*. 2004). The micrite lamina with alpha fabric components suggest rapid precipitation from evaporated or

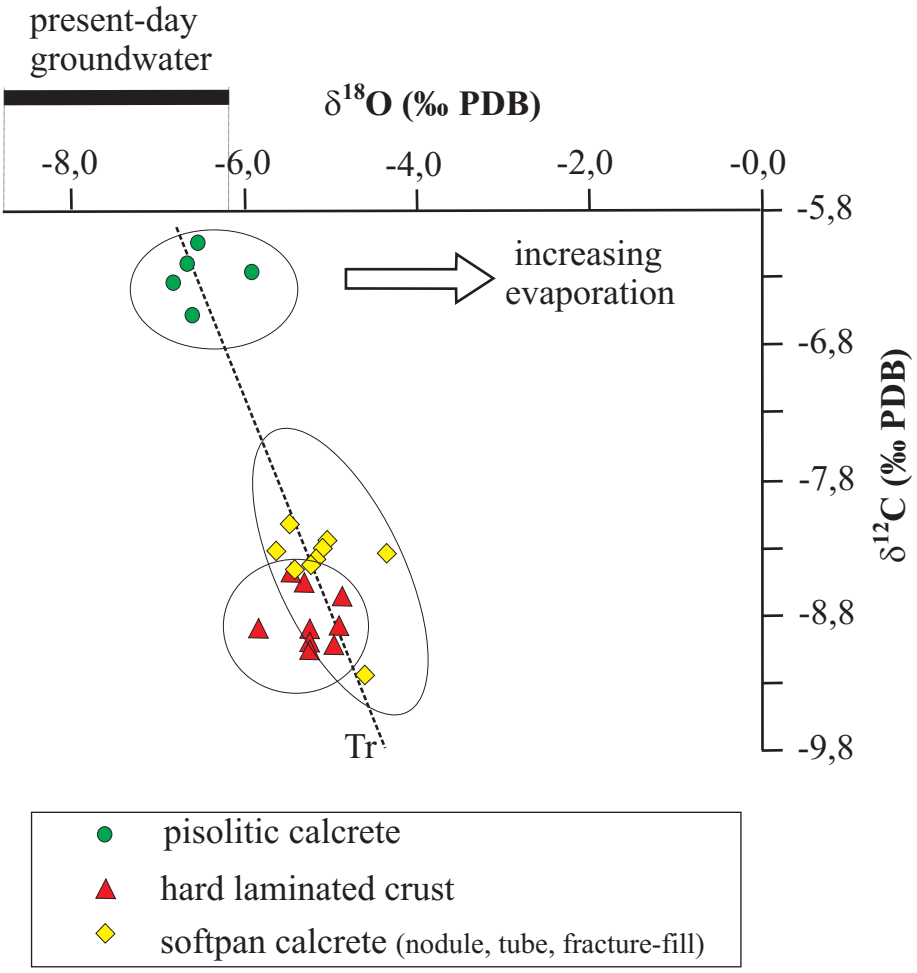

Figure 7. A crossplot of stable isotope values of the studied calcretes and present–day groundwater (Hatipoğlu 2004), using conversion of Hut (1987). A rough inverse covariation (Tr) between $\delta^{18}O$ and $\delta^{13}C$ values is observed.

supersaturated meteoric water (Harrison 1977; Braithwaite 1979), which is also evidenced by the $\delta^{18}O$ values. Replacive/displacive features of calcite are also common, taking place from supersaturated water (Watts 1980). The calcite $\delta^{13}C$ values indicate a contribution of light CO_2 released from the soil into percolating water. The soil formation is proved by the abundance of beta-fabric components such as rhizoliths, microbial structures (calcified filaments, calcite needles, spherical calcite bodies), alveolar texture and vadose calcrete pisoliths which are strong evidence of biological activity. The plant roots act as conduits for calcium-rich water and also provide sites at which fungi and bacteria thrive (Jones & Ng 1988) which are important in triggering carbonate precipitation (Callot *et al.* 1985; Chafetz 1986; Phillips & Self 1987). The macro- and micro-organisms have played direct or indirect roles in the dissolution and precipitation of calcium carbonate such as providing light CO_2, weathering, evapotranspiration and biomineralization. The micrite coatings around the root traces and cellular cortex structure may suggest calcite precipitation and/or absorbtion on the root-surface from the run-off water when the root was alive. The same process is also considered for the calcification of micro-organisms. Calcite precipitation also continued after root-decay which is represented by root-casts. In the field, the presence of rhizolithic mat and residual soil in the hard laminated crust point to a major interruption in the hard laminated crust

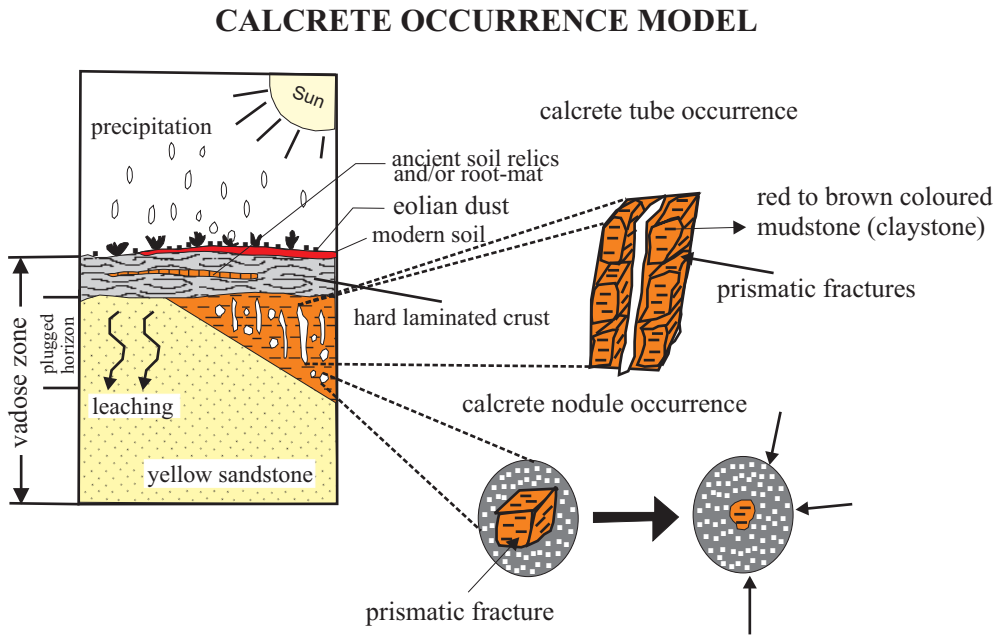

Figure 8. A schematic presentation of calcrete formation.

development, indicating episodic climate change (Candy *et al*. 2004). The calcrete crusts were developed by the vertical accretion from bottom to top, as suggested by their setting over the plugged horizon and presence of rhizolithic mat and residual soil in the hard laminated crust (Lal & Kimble 2000).

The third stage is characterized by a pisolithic crust in which pisoliths are inversely graded and poorly sorted, and show light and dark concentric wavy lamination around a nucleus. The laminae are prodominantly micrite. Their bedded character with the other features suggest that they were moving around when the micrite was precipitating around nuclei (Read 1974; Arakel 1982; Nash & McLaren 2003; Fu *et al*. 2004). By rolling, they were transported and then accumulated in troughs among the dome-like structures. The gravity and surface water caused movement of pisoliths on slopes of dome-like structures. The slightly more negative calcite $\delta^{18}O$ values and less negative calcite $\delta^{13}C$ values of the pisoliths reveal input of rain-water, and relatively less influence from soil-water.

Overall, calcretes in the Mersin area are pedogenic (soil related) in origin and formed by soil processes which are characterized by beta fabric components and negative calcite $\delta^{13}C$ values. Pedogenic calcretes are well documented in the literature (Gile *et al*. 1966; Watts 1980; Arakel 1982; Wright & Tucker 1991; Wright *et al*. 1995; Fu *et al*. 2004). The soil processes released light-CO_2 into the meteoric percolating water that resulted in vertical and lateral redistribution of dissolved calcium carbonate that later precipitated from supersaturated water as microcrystalline calcite and replaced the host rocks/sediments from the same fluid. In the sites of extensive calcification, the host-rocks/sediments show a colour change from reddish brown to greenish grey due to removal of hematite pigment by infiltrating water (Figures 4d, g & i). Alternating wet and dry periods are very important for calcrete formation, and characteristic of arid and semi-arid climates. The wet periods caused population of macro and micro-organisms that contributed to the soil-formation and dissolution of calcium carbonate. The following dry periods increased the calcium concentration in the soil-derived water from calcium carbonate precipitated by evapotranspiration and degassing of CO_2 and also calcium carbonate replaced/displaced the host rocks or sediments. The source of calcite is considered to be detrital carbonate, eolian dust and calcrete carbonate material itself. During the dry periods, the palygorskite formed from strongly evaporated percolating water after or during calcite precipitation under alkaline conditions

with high pH (~8–11), high Si, Mg and low Al ion activities (Singer & Norrish 1974; Verrecchia & Le Coustumer 1996; Colson *et al*. 1998; Akbulut & Kadir 2003). The Al, Si and Mg were derived possibly from smectite clay minerals which are dominant in the host rocks/sediments.

Conclusion

Calcretes in the Mersin district are pedogenic in origin based on the abundance of beta-fabric constituents and negative calcite $\delta^{13}C$ values indicate significant contributions of soil-derived CO_2. They occurred in the vadose zone, were deposited from percolating meteoric water and exhibit various forms within the several calcrete profiles. The calcrete morphology changes with time related to stages of their development characterized by a mottling or plugged horizon including isolated calcrete forms, calcrete crusts and a pisolithic crust.

Acknowledgements

This study was financially supported by the Scientific and Techological Research Council of Turkey (TÜBİTAK) under the Project of YDABAG-102Y036. Therefore, the authors are grateful to TÜBİTAK for its support. We thank Professor Dr. Maurice E. Tucker and anonymous reviewer of the journal for their constructive reviews. Chris Herron and Steve Mittewede edited English of the text. Thanks are also due to John D.A. Piper for his kind help in polishing the English of the final text.

References

Akbulut, A. & Kadir, S. 2003. The geology and origin of sepiolite, palygorskite and saponite in Neogene lacustrine sediments of the Serinhisar-Acıpayam Basin, Denizli, SW Turkey. *Clays and Clay Minerals* **51**, 279–292.

Alonso-Zarza, A.M. & Arenas, C. 2004. Cenozoic calcretes from the Teruel Graben, Spain: microstructure, stable isotope geochemistry and environmental significance. *Sedimentary Geology* **167**, 91–108.

Arakel, A.V. 1982. Genesis of calcrete in Quaternary soil profiles. Hutt and Leeman lagoons, Western Australia. *Journal of Sedimentary Petrology* **52**, 109–125.

Arakel, A.V. & McConchie, D. 1982. Classification and genesis of calcrete and gypsite lithofacies in paleodrainage systems of Inland Australia and their relationship to Carnotite mineralization. *Journal of Sedimentary Petrology* **52**, 1149–1170.

Atabey, E., Atabey, N. & Kara, H. 1998. Sedimentology of caliche (calcrete) occurrences of the Kırşehir region. *Mineral Research and Exploration Institute (MTA) of Turkey Bulletin* **120**, 69–80.

Atalay, I. 1996. Palaeosols as indicators of the climatic changes during Quaternary period in S Anatolia. *Journal of Arid Environments* **32**, 23–35.

Bajnoczi, B. & Kovacs-Kis, V. 2006. Origin of pedogenic needle-fiber calcite revealed by micromorphology and stable isotope composition – a case study of a Quaternary paleosol. *Chemie der Erde Geochemistry* **66**, 203–212.

Braithwaite, C.J.R. 1979. Crystal textures of recent fluvial pisolites and laminated crystalline crusts in Dyfed, South Wales. *Journal of Sedimentary Petrology* **49**, 181–193.

Brindley, G.W. 1980. Quantitative X-ray analyses of clays. *In:* Brindley, G.W. & Brown, G. (eds), *Crystal Structures of Clay Minerals and Their X-ray Identification*. Mineralogical Society Monograph **5**, London, 411–438.

Callot, G., Guyon, A. & Mousain, D. 1985. Interrelations entre aiguilles de calcite et hyphes myceliens. *Agronomie* **5**, 209–216.

Calvet, F. 1982. Constructive micrite envelopes developed in vadose continental environments in Pleistocene eolianites of Mallorca (Spain). *Acta Geologica Hispanica* **17**, 169–178.

Calvet, F. & Julia, R. 1983. Pisoids in the caliche profiles of Tarragona, Northeast Spain. *In:* Peryt, T.M. (ed), *Coated Grains*. Springer, Berlin, 456–473.

Candy, I., Black, S. & Sellwood, B.W. 2004. Quantifiying time scale of pedogenic calcrete formation using U-series disequilibria. *Sedimentary Geology* **170**, 177–187.

Chafetz, H.S. 1986. Marine peloids: a product of bacterially induced precipitation of calcite. *Journal of Sedimentary Petrology* **56**, 812–817.

Cerling, T.E. 1984. The stable isotopic composition of modern soil carbonate and its relationship to climate. *Earth and Planetary Science Letters* **71**, 229–240.

Colson, J., Cojan, I. & Thiry, M. 1998. A hydrogeological model for palygorskite formation in the Danian continental facies of the Provence Basin (France). *Clay Minerals* **33**, 333–347.

Demicco, R.V. & Hardie, L.A. 1994. *Sedimentary Structures and Early Diagenetic Features of Shallow Marine Carbonate Deposits*. Society of Economic Paleontologists and Mineralogists, Atlas Series **1**, Society of Sedimentary Geology, Tulsa.

Eren, M. 2007. Genesis of tepees in the Quaternary hardpan calcretes, Mersin, S Turkey. *Carbonates and Evaporites* **22**, 123–134.

Eren, M. & Kadir, S. 1999. Colour origin of upper Cretaceous pelagic red sediments within the Eastern Pontides, northeast Turkey. *International Journal of Earth Sciences* **88**, 593–595.

Esteban, M. 1974. Caliche textures and Microcodium. *Societa Geologica Italiana Bolettino* **92**, 105–125.

ESTEBAN, M. & KLAPPA, C.F. 1983. Subaerial exposure environment. *In*: SCHOLLE, P.A., BEBOUT, D.G. & MOORE, C.H. (eds), *Carbonate Depositional Environments*. Association of American Petroleum Geologists Memoir **33**, Tulsa, Oklahoma, 1–54.

FLUGEL, E. 2004. *Microfacies of Carbonate Rocks: Analysis, Interpretation and Application*. Springer, Berlin-Heidelberg.

FU, Q., QING, H. & BERGMAN, K.M. 2004. Dolomitized calcrete in the Middle Devonian Winnipegosis carbonate mounds, subsurface of South-central Saskatchewan, Canada. *Sedimentary Geology* **168**, 49–69.

GILE, L.H., HAWLEY, J.W. & GROSSMAN, R.B. 1981. *Soils and Geomorphology in the Basin and Range Area of Southern New Mexico*. Guidebook to the Desert Project-Memoir **39**, New Mexico Bureau of Mines and Mineral Resources, Socorro-New Mexico.

GILE, L.H., PETERSEN, F.F. & GROSSMAN, R.S. 1966. Morphological and genetic sequences of carbonate accumulation in desert soils. *Soil Science* **101**, 347–360.

GONG, S.Y., MII, H.S., WEI, K.Y., HORNG, C.S., YOU, C.F., HUANG, F.W., CHI, W.R., YUI, T.Z., TORNG, P.K., HUANG, S.T., WANG, S.W., WU, J.C. & YANG, K.M. 2005. Dry climate near the Western Pacific Warm Pool: Pleistocene caliches of the Nansha Islands, South China Sea. *Palaeogeography, Palaeoclimatology, Palaeoecology* **226**, 205–213.

GOUDIE, A.S. 1973. *Duricrusts in Tropical Landscapes*. Clarendon Press, Oxford.

GOUDIE, A.S. 1983. Calcrete. *In:* GOUDIE, A.S. & PYE, K. (eds), *Chemical Sediments and Geomorphology*. Academic Press, London, 93–131.

GOUDIE, A.S. 1996. Organic agency in calcrete development. *Journal of Arid Environments* **32**, 103–110.

HARRISON, R.S. 1977. Caliche profiles: indicators of near-surface subaerial diagenesis, Barbados, West Indies. *Bulletin of Canadian Petroleum Geology* **25**, 123–173.

HATİPOĞLU, Z. 2004. *Hydrogeochemistry of Mersin-Tarsus Coastal Aquifer*. PhD Thesis, Hacettepe University, Ankara, Turkey [in Turkish with English abstract, unpublished].

HAY, R.L. & REEDER, R.J. 1978. Calcretes of Olduvai Gorge and the Ndolanya Beds of northern Tanzania. *Sedimentology* **25**, 649–672.

HUT, G. 1987. *Stable Isotope Reference Samples for Geochemical and Hydrological Investigations*. In Report of the Director General, IAEA, Vienna.

JAMES, N.P. 1972. Holocene and Pleistocene calcareous crust (caliche) profiles: criteria for subaerial exposure. *Journal of Sedimentary Petrology* **42**, 817–836.

JAMES, N.P. & CHOQUETTE, P.W. 1984. Diagenesis 9. Limestones - the meteoric diagenetic environment. *Geoscience Canada* **11**, 161–194.

JIMENEZ DE CISNEROS, C., MOLINA, J.M., NIETO, L.M., RUIZ-ORTIZ, P.A. & VERA, J.A. 1993. Calcretes from a palaeosinkhole in Jurassic palaeokarst (Subbetic, southern Spain). *Sedimentary Geology* **87**, 13–24.

JIMENEZ-ESPINOSA, R. & JIMENEZ-MILLAN, J. 2003. Calcrete development in Mediterranean colluvial carbonate systems from SE Spain. *Journal of Arid Environments* **53**, 479–489.

JONES, B. & NG, K.C. 1988. The structure and diagenesis of rhizoliths from Cayman Brac, British West Indies. *Journal of Sedimentary Petrology* **58**, 457–467.

KAPUR, S., ÇAVUŞGİL, V.S. & FITZPATRICK, E.A. 1987. Soil-calcrete (caliche) relationship on a Quaternary surface of the Cukurova Region, Adana (Turkey). *In:* FEDEROFF, N., BRESSON, L.M. & COURTY, M.A. (eds), *Soil Micromorphology*. Association Française pour L'Etude du sol, Paris, 597–603.

KAPUR, S., ÇAVUŞGİL, V.S., ŞENOL, M., GÜREL, N. & FITZPATRICK, E.A. 1990. Geomorphology and pedogenic evolution of Quaternary calcretes in the northern Adana Basin of southern Turkey. *Zeitschrift für Geomorphologie* **34**, 49–59.

KAPUR, S., SAYDAM, C., AKÇA, E., ÇAVUŞGİL, V.S., KARAMAN, C., ATALAY, I. & ÖZSOY, T. 2000. Carbonate pools in soil of the Mediterranean: a case study from Anatolia. *In:* LAL, R., KIMBLE, J.M., ESWARAN, H. & STEWART, B.A. (eds), *Global Climate Change and Pedogenic Carbonates*. Lewis Publishers, Boca Raton, Florida, 187–212.

KAPUR, S., YAMAN, S., GÖKÇEN, S.L. & YETİŞ, C. 1993. Soil stratigraphy and Quaternary caliche in the Misis area of the Adana Basin, southern Turkey. *Catena* **20**, 431–445.

KHADKIKAR, A.S., MERH, S.S., MALIK, J.N. & CHAMYAL, L.S. 1998. Calcretes in semi-arid alluvial systems: formative pathways and sinks. *Sedimentary Geology* **116**, 251–260.

KLAPPA, C.F. 1978. Biolithogenesis of Microcodium: elucidation. *Sedimentology* **25**, 489–522.

KLAPPA, C.F. 1979. Calcified filaments in Quaternary calcretes: organo-mineral interactions in the subaerial vadose environment. *Journal of Sedimentary Petrology* **49**, 955–968.

KLAPPA, C.F. 1980. Rhizoliths in terrestrial carbonates: classification, recognition, genesis and significance. *Sedimentology* **27**, 613–629.

KNAUTH, L.P., BRILLI, M. & KLONOWSKI, S. 2003. Isotope geochemistry of caliche developed on basalt. *Geochimica et Cosmochimica Acta* **67**, 185–195.

KNOX, G.J. 1977. Caliche profile formation, Saldanha Bay (South Africa). *Sedimentology* **24**, 657–674.

LAL, R. & KIMBLE, J.M. 2000. Pedogenic carbonates and the global carbon cycle. *In:* LAL, R., KIMBLE, J.M., ESWARAN, H. & STEWARD, B.A. (eds), *Global Climate Change and Pedogenic Carbonates*. Lewis, Boca Raton, 1–14.

LEE, Y.II. 1999. Stable isotopic composition of calcic paleosols of the Early Cretaceous Hasandong Formation, southeastern Korea. *Palaeogeography, Palaeoclimatology, Palaeoecology* **150**, 123–133.

MOORE, D.M. & REYNOLDS, R.C. 1989. *X-ray Diffraction and the Identification and Analysis of Clay Minerals*. Oxford University Press, Oxford.

NASH, D.J. & MCLAREN, S.J. 2003. Kalahari valley calcretes: their nature, origins, and environmental significance. *Quaternary International* **111**, 3–22.

ÖZER, A.M., WIESER, A., GÖKSU, H.Y., MÜLLER, P., REGULLA, D.F. & EROL, O. 1989. ESR and TL age determination of caliche nodules. *International Journal of Radiation Applications and Instrument. Part A- Applied Radiation and Isotopes* **40**, 1159–1162.

PAQUET, H. & RUELLEN, A. 1997. Calcareous epigenetic replacement (epigenie) in soils and calcrete formation. *In:* PAQUET, H. & CLAUER, N. (eds), *Soils and Sediments–Mineralogy and Geochemistry*. Springer,Berlin Heidelberg, 21–48.

PHILLIPS, S.E., MILNES, A.R. & FOSTER, R.C. 1987. Calcified filaments: an example of bilogical influences in the formation of calcrete in South Australia. *Australian Journal of Soil Research* **25**, 405–428.

PHILLIPS, S.E. & SELF, P.G. 1987. Morphology, crystallography and origin of needle-fibre calcite in Quaternary pedogenic carbonates of South Australia. *Australian Journal of Soil Research* **25**, 429–444.

PURVIS, K. & WRIGHT, V.P. 1991. Calcretes related to phreatophytic vegetation from the Middle Triassic Otter Sandstone of South West England. *Sedimentology* **38**, 539–551.

RAO, V.P. 1990. On the occurrence of caliche pisolites from the western continental shelf of India. *Sedimentary Geology* **69**, 13–19.

READ, J.F. 1974. Calcrete deposits and Quaternary sediments, Edel Province, Shark Bay, Western Australia. *American Association of Petroleum Geologists Memoir* **22**, 250–282.

REEVES, C.C.Jr. 1970. Origin, classification, and geologic history of caliche on the Southern High Plains, Texas and Eastern New Mexico. *Journal of Geology* **78**, 352–362.

ROBINSON, S.A., ANDREWS, J.E., HESSELBO, S.P., RADLEY, J.D., DENNIS, P.F., HARDING, I.C. & ALLEN, P. 2002. Atmospheric pCO_2 and depositional environment from stable-isotope geochemistry of calcrete nodules (Barremian, Lower Cretaceous, Wealden Beds, England). *Journal of the Geological Society, London* **159**, 215–224.

ROSSINSKY, V. & WANLESS, H.R. 1992. Topographic and vegetative controls on calcrete formation, Turks and Caicos Islands, British West Indies. *Journal of Sedimentary Petrology* **62**, 84–98.

SANCHO, C., MELENDEZ, A., SIGNES, M. & BASTIDA, J. 1992. Chemical and mineralogical characteristics of Pleistocene caliche deposits from the central Ebro Basin, NE Spain. *Clay Minerals* **27**, 293–308.

SHAABAN, M.N. 2004. Diagenesis of the lower Eocene Thebes Formation, Gebel Rewagen area, Eastern Desert, Egypt. *Sedimentary Geology* **165**, 53–65.

SINGER, A. & NORRISH, K. 1974. Pedogenic palygorskite occurrences in Australia. *American Mineralogist* **59**, 508–517.

STRONG, G.E., GILES, J.R.A. & WRIGHT, V.P. 1992. A Holocene calcrete from North Yorkshire, England: implications for interpreting palaeoclimates using calcretes. *Sedimentology* **39**, 333–347.

TANDON, S.K. & ANDREWS, J.E. 2001. Lithofacies associations and stable isotopes of palustrine and calcrete carbonates: examples from an Indian Maastrichtian regolith. *Sedimentology* **48**, 339–355.

TUCKER, M.E. 1991. *Sedimentary Petrology: An Introduction to the Origin of Sedimentary Rocks*. Blackwell Science, Oxford.

TUCKER, M.E. & WRIGHT, V.P. 1990. *Carbonate Sedimentology*. Blackwell Science, Oxford.

VAN HOUTEN, F.B. 1973. Origin of red beds: a review – 1961–1972. *Annual Review Earth and Planetary Sciences* **1**, 39–61.

VERRECCHIA E.P., DUMONT, J.L. & VERRECCHIA, K.E. 1993. Role of calcium oxalate biomineralization by fungi in the formation of calcretes: a case study from Nazareth, Israel. *Journal of Sedimentary Petrology* **63**, 1000–1006.

VERRECCHIA, E.P. & LE COUSTUMER, M.N. 1996. Occurrence and genesis of palygorskite and associated clay minerals in a Pleistocene calcrete complex, SDE Boqer, Negev Desert, Israel. *Clay Minerals* **31**, 183–202.

WALLS, R.A., HARIS, W.B. & NUNAN, W.E. 1975. Calcareous crust (caliche) profiles and early subaerial exposure of Carboniferous carbonates, northeastern Kentucky. *Sedimentology* **22**, 417–440.

WANG, Y., NAHON, D. & MERINO, E. 1994. Dynamic model of the genesis of calcrete replacing silicate rocks in semi-arid regions. *Geochimica et Cosmochimica Acta* **58**, 5131–5145.

WARD, W.C. 1975. Petrology and diagenesis of carbonate eolianites of northeastern Yucatan Peninsula, Mexico. *In:* WONTLAND, K.F. & PUSEY, W.C. III (eds), *Belize Shelf-Carbonate Sediments. Clastic Sediments and Ecology*. Tulsa, Oklahoma, American Association of Petroleum Geologists, 500–571.

WATTS, N.L. 1980. Quaternary pedogenic calcretes from the Kalahari (southern Africa): mineralogy, genesis and diagenesis. *Sedimentology* **27**, 661–686.

WRIGHT, V.P. 1986. The role of fungal biomineralization in the formation of early Carboniferous soil fabrics. *Sedimentology* **33**, 831–838.

WRIGHT, V.P., PLATT, N.H., MARRIOTT, S.B. & BECK, V.H. 1995. A classification of rhizogenic (root-formed) calcretes, with examples from the Upper Jurassic–Lower Cretaceous of Spain and Upper Cretaceous of southern France. *Sedimentary Geology* **100**, 143–158.

WRIGHT, V.P., PLATT, N.H. & WIMBLEDON, W.A. 1988. Biogenic laminar calcretes: evidence of calcified root-mat horizons in paleosols. *Sedimentology* **35**, 603–620.

WRIGHT, V.P. & TUCKER, M.E. 1991. *Calcretes*. Blackwell Scientific Publications, Oxford.

YALÇIN, M.N. & GÖRÜR, N. 1983. Sedimentological evolution of the Adana Basin. *In:* TEKELİ, O. & GÖNCÜOĞLU, M.C. (eds), *Geology of the Taurus Belt*. Proceedings of International Tauride Symposium. Mineral Research and Exploration Institute (MTA) of Turkey Publications, 165–172.

YETİŞ, C. 1988. Reorganization of the Tertiary stratigraphy in the Adana Basin, southern Turkey. *Stratigraphy Newsletters* **20**, 43–58.

YETİŞ, C., KELLING, G., GÖKÇEN, S.L. & BAROZ, F. 1995. A revised stratigraphic framework for later Cenozoic sequences in the northeastern Mediterranean region. *Geologishe Rundschau* **84**, 794–812.

Received 13 November 2007; revised typescript received 21 January 2008; accepted 11 February 2008